

Article

Performance Improvement of Axial Flux Permanent Magnet Machine with Phase Group Concentrated Coil Winding

Muhammad Ramiz Zakir ¹, Junaid Ikram ¹, Saleem Iqbal Shah ¹, Syed Sabir Hussain Bukhari ², Salman Ali ^{3,*}  and Fabrizio Marignetti ^{3,*} 

¹ Department of Electrical and Computer Engineering, COMSATS University, Islamabad 45550, Pakistan

² Department of Electrical Engineering, Sukkur IBA University, Sukkur 65200, Pakistan

³ Department of Electrical and Information Engineering, University of Cassino and Southern Lazio, 03043 Cassino, Italy

* Correspondence: salman.ali@unicas.it (S.A.); marignetti@unicas.it (F.M.)

Abstract: This paper suggests a method to improve the performances of the Dual Stator Axial Flux Spoke-type Permanent Magnet (DSAFSPM) machines with phase group concentrated coil (PGCC) windings, by incorporating continuous and discrete step-skewing along with a special winding connection. The purpose of the study is to mitigate the cogging torque and torque ripples while increasing the output torque so it ameliorates the machine performance at minimum cost for various applications such as wind power plants and electric vehicles (EVs). Cogging torque produces noise and vibrations which degrade the machine's performance and reduces its life span. The proposed winding sequence enhances the output torque by improving its distribution factor along with the use of continuous skew and step-skew magnets. This research work improved the cogging torque and torque ripples with the help of skew techniques while output torque is increased by the proposed winding sequence. Further harmonics and ripples are also mitigated by the proposed winding sequence. The overall machine volume is kept constant along with the magnet size and the design parameters for fair performance analysis. Comparative analysis of these machines is performed using three-dimensional (3-D) time-stepped finite element analysis (FEA). Proposed model I and proposed model II reduce the harmonics by 42% and 23%, respectively. By using continuous skew and discrete step-skew magnets, cogging torque is reduced up to 81.5% and 75%, respectively. This reduction in cogging torque reduces the noise and vibration in machines which assists the machines to perform a smooth operation. The reduction in output torque ripples in proposed model I is 60.8% while that of proposed model II is 59.3%.



Citation: Zakir, M.R.; Ikram, J.; Shah, S.I.; Bukhari, S.S.H.; Ali, S.; Marignetti, F. Performance Improvement of Axial Flux Permanent Magnet Machine with Phase Group Concentrated Coil Winding. *Energies* **2022**, *15*, 7337. <https://doi.org/10.3390/en15197337>

Academic Editor: Nicu Bizon

Received: 1 September 2022

Accepted: 1 October 2022

Published: 6 October 2022

Publisher's Note: MDPI stays neutral with regard to jurisdictional claims in published maps and institutional affiliations.



Copyright: © 2022 by the authors. Licensee MDPI, Basel, Switzerland. This article is an open access article distributed under the terms and conditions of the Creative Commons Attribution (CC BY) license (<https://creativecommons.org/licenses/by/4.0/>).

1. Introduction

Axial flux permanent magnet machines (AFPMM) produce relatively higher torque at lower speed and have a compact structure and smaller weight-to-size ratio which makes them suitable for high torque density applications [1]. Axial flux machines are vastly being used in wind power generation and electric vehicles (EVs) due to their numerous benefits as compared to radial flux machines [2]. Furthermore, using AFPMM allows for reducing the mechanical structure complexity as it reduces the need for a gearbox [3].

In different applications such as wind power generation and EVs, the torque ripple mitigation technique is required to perform smooth and uninterrupted operations with increased output torque at minimum cost [4]. Along with its various advantages, AFPMM exhibits torque ripples and cogging torque [5]. The presence of torque ripples causes mechanical vibrations that ultimately generate vibro-acoustic behavior and reduce the life span of machines [6]. Torque ripples are mainly due to the cogging torque and non-sinusoidal back EMF in the machine. Cogging torque in permanent magnet machines is due

to magnetic interaction between stator teeth and rotor poles [7–10]. The cost of the AFPMM mainly depends on the cost of the permanent magnets (PMs) [11]. Ferrite PMs reduce the cost of the machine as compared to rare earth PMs at the expense of the reduction in the output torque. So, it is mandatory to utilize some technique to increase output torque when ferrite PMs are used [12].

The dual stator spoke-type AFPM increases the torque output with reduced cost by the integration of two stators as compared to the single stator AFPM, due to the flux focusing effect but this structure also increases the cogging torque and torque ripples in the machine [13]. The spoke-type configuration improves the air gap flux density and the torque density in the machine [14]. The dual stator AFPMs with phase group concentrated coil (PGCC) winding enhances the output torque as compared to the simply concentrated winding to acquire the unity winding factor and remarkable fault-tolerant capabilities [15]. PGCC winding, together with the spoke-type rotor configuration, enhances the flux focusing effect in the machine, thus compensating for the inferior ferrite magnetic properties [16]. However, the flux-focusing spoke-type rotor configuration enhances the torque ripples in the machine [17].

An unaligned stator shifted by one stator tooth width in spoke-type dual stator AFPMMs, reduces the cogging torque at the price of reducing air gap magnetic flux density as compared to dual axial aligned stators [18]. Cogging torque and torque ripples in axial flux PM machines are reduced with the help of the poles skewing technique [19]. Poles skewing is one of the most effective techniques to mitigate the cogging torque and the torque ripples at the rotor side. In AFPMM, step-skewed rotor (SSR) performance and structure are better than stator slots skewed motor. SSR is capable of reducing harmonics significantly even with a few steps [20]. Rotor side modifications reduce the design complexities as compared to stator side modifications. With rotor skew configuration we avoid many complications that are faced in stator skewing [21]. Furthermore, SSR configuration significantly mitigates the problems related to the voltage harmonics distortion that consequently ameliorates the back EMF and torque ripples in the machine [14].

In APMMs, choosing a suitable skew angle can significantly reduce the components of a particular time harmonic [22]. The skew rotor technique mitigates the cogging torque and torque ripples in the motor, suppressing the vibro-acoustic behavior due to the reduction in specific time harmonic components [23]. Most of the harmonic components can be suppressed by adopting an optimal skew angle in step-skew rotor configuration. Further, an increase in skew angle reduces the noise but decreases significantly the output torque, so it is necessary to choose skew angle carefully [8,24].

This research work uses a combination of PGCC windings and continuous skewed trapezoidal PMs as well as step-skewed PMs to enhance the performance of the dual stator axial flux spoke-type PM machine (DSAFSPMM). DSAFSPMM with trapezoidal PMs is named as conventional model. DSAFSPMM with continuous trapezoidal skewed PMs is named proposed model I. DSAFSPMM with stepped skewed trapezoidal PMs is labeled as proposed model II. Proposed model I, as well as proposed model II, reduce the harmonics significantly. Reduction in harmonics is mainly due to the change of the relative position between rotor PMs and stator teeth. Proposed model II is slightly more cost-effective as compared to proposed model I as the magnets have a simpler shape and can be placed with the use of spacers. Moreover, magnet loss in segmented magnets is lower.

Finally, changing the phase sequence of the windings also improves the performance of the DSAFSPMM. This proposed winding sequence limits the aforementioned issues that occurred in the conventional model. The performance of the proposed winding sequence is analyzed with the conventional model, proposed model I, and proposed model II. By using the proposed winding sequence, torque ripples are decreased, and the output torque is increased. The proposed winding sequence enhances the output torque by improving its distribution factor which ultimately improves the winding factor. All the dimensions, materials, and design parameters in the investigated machines are kept the

same to obtain a fair comparison. Time-stepped 3D Finite Element Analysis (FEA) is used for the comparative analysis.

This research work is organized as follows: Section 2 explains the comparison of conventional and proposed magnets as well as describes the flux path of conventional and proposed machines. Section 3 describes the comparative analysis among conventional DSAFSPMM and proposed models of DSAFSPMM having continuous and discrete step-skewed PMs. Furthermore, this section describes further enhancement by using switched phase sequence. In the end, a comparison of results is encapsulated in Section 4.

2. Conventional and Proposed Models

This section compares the conventional trapezoidal PMs, skewed trapezoidal PMs and discrete stepped skewed PMs. The conventional trapezoidal PMs, proposed skewed trapezoidal PMs and discrete stepped skewed PMs are shown in Figures 1–3 and are labeled here as conventional PM, Proposed PM I, and Proposed PM II, respectively. The conventional model, proposed model I and proposed model II of the DSAFSPMM are also covered in this section.

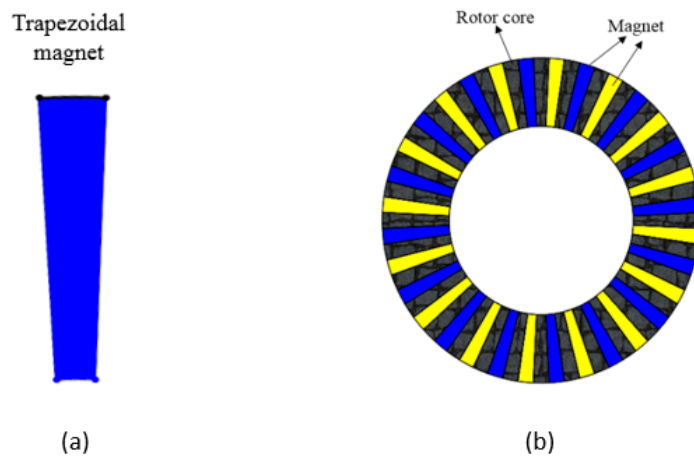


Figure 1. Conventional model PM shape: (a) Trapezoidal magnet; (b) Trapezoidal magnets and rotor core.

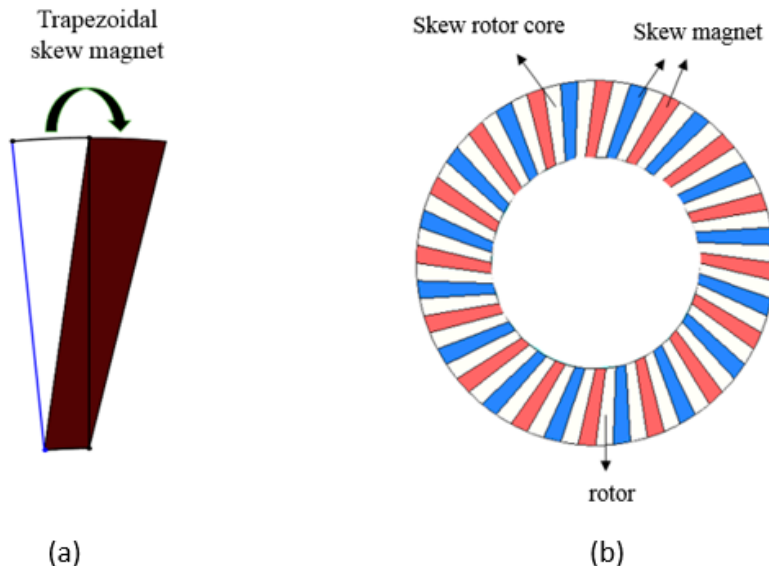


Figure 2. Proposed model I PM shape: (a) Trapezoidal skew magnet; (b) Trapezoidal skew magnets and rotor core.

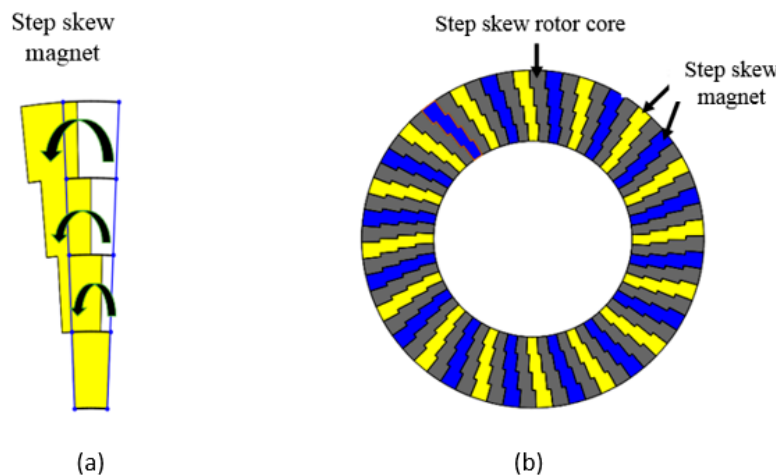


Figure 3. Proposed model II PM shape: (a) Step-skew magnet (built-in skew); (b) Step-skew magnets and rotor core.

2.1. Comparison of the Conventional PM, Proposed PM I, and Proposed PM II

The trapezoidal PM is used in the conventional model. Proposed PM I is a continuous trapezoidal skewed PM. The skew angle in proposed PM I is the ratio of 360° to the rotor pole pitch [11]. This optimal skew angle mitigates the torque ripples and cogging torque significantly.

$$\theta_{skew} = \frac{2\pi}{\text{no of rotor poles}} = \frac{360}{N_r} \quad (1)$$

Proposed PM II is a discrete step-skewed PM. The overall skew angle of proposed PM I and PM II is the same. Proposed PM II has four steps in shape which are shifted from each other by a step angle. The step angle is determined by the ratio of the skew angle to the number of steps. Therefore, as each step of the magnet is shifted at a constant angle, this is also called a built-in skew magnet. The volume, axial thickness, and width of the magnet are kept constant in all three models. PMs are magnetized in alternate outward; inward magnetization directions and a circumferential anisotropic pattern is applied. The design parameters of the machines are shown in Table 1.

Table 1. Design parameters of conventional model, proposed model I and proposed model II.

Items	Symbols	Unit	Value
Number of stator slots	Q	-	30
Number of magnet poles	2P	-	32
Stator/rotor outer diameter	D _o	mm	300
Stator/rotor inner diameter	D _i	mm	174
Total axial length	L _s	mm	72
Magnet span	M _w	degree	11.25
Magnet skew (Trap)	α	degree	5.625
Magnet skew (Step)	α	degree	1.40625
Air gap	g	mm	1.0
Stator tooth height	h _t	mm	19
Stator yoke height	h _y	mm	5
Rotor/PM height	h _r	mm	22

Table 1. Cont.

Items	Symbols	Unit	Value
Length of the Magnet	L_m	mm	63
Number of turns per coil	N_c	-	36
Connection	Y	-	Wye
Remanence of ferrite PM	B_r	T	0.43
No of slots/phase belt	m	-	2
Coil spacing of different phase belt (conventional)	β_1	elec degree	88
Coil spacing of different phase belt (proposed)	β_2	elec degree	32
Distribution factor for conventional sequence	K_{d1}	degree	0.7192
Distribution factor for proposed sequence	K_{d2}	degree	0.9613
Rotor	-	-	50H470
Stator	-	-	50H470
Magnet	-	-	Ferrite
Coil	-	-	Copper

The cogging torque is due to the change in reluctance between the stator slots and the permanent magnets. The conventional model magnets are skewed to mitigate the cogging torque (T_{cog}) and are named as a proposed model I that is utilizing continuous trapezoidal skew magnet while in proposed model II, magnets are skewed in the form of discrete steps that comprises built-in skew in magnets with constant distance in each step. The number of these steps can be increased to obtain the minimum cogging torque but at the cost of a reduction in output torque. So, the optimal number of steps is selected to obtain the desired results. This discrete step-skew magnet has varying skew angles from the first step to the fourth step in magnet shape. By adjusting the number of steps, cogging torque amplitude can be minimized and maximized. Cogging torque is directly related to flux density as shown in Equation (2).

$$T_{cog} = -\frac{1}{2}\Phi_g^2 \frac{dR}{d\theta} \quad (2)$$

where Φ_g is denoting air gap flux density and $\frac{dR}{d\theta}$ is denoting the change in reluctance with respect to the rotor position. This cogging torque occurs periodically due to periodic variations in air-gap reluctance. Due to this periodicity, cogging torque can be represented in the form of the Fourier series:

$$T_{cog} = \sum_{k=1}^{\infty} T_{mk} \sin(mk\theta) \quad (3)$$

where m denotes the least common multiple of the number of stator slots and number of poles, while k is an integer. T_{mk} denotes the Fourier coefficient. Equation (3) shows that in one mechanical revolution, cogging torque has m periods. So, it is adding up the harmonic sinusoids. When there is no cogging torque and torque ripples mitigation technique in the machine, then the additive effect occurs for each rotor magnet on the cogging torque due to the same relative position of each magnet with respect to the stator slots. It leads toward the summation of harmonic components because the resultant torque from each magnet is in phase. Some of the harmonic components can be eliminated when the cogging effect from each magnet is out of phase and it is achieved by imposing continuous skew and discrete step-skew techniques.

The performance is improved significantly by imposing a continuous skew magnet in the machine and achieving equivalent results as in the discrete step-skew magnet. However, the continuous skewing technique leads toward an irregular magnet shape that is difficult to magnetize and fabricate which makes continuous skewing complex and costly. The step-skewing of magnets resolves the aforementioned issues of continuous skewing. So, the continuous skewing technique is better than no skew magnets but the discrete step-skewing technique is preferable to the continuous skewing technique. When these techniques are used alone, they also affect the output torque. Whereas the reluctance is due to the opposition of flux between rotor poles and stator slots and it always changes with respect to the rotor position. It is directly proportional to the length of flux flowing path and inversely proportional to the cross-sectional area and it can be written as

$$R = \frac{l}{\mu_0 A} \quad (4)$$

where l denotes the length of the magnetic path, μ_0 is the permeability of free space and A is the cross-sectional area. At some instants, rotor poles are facing stator teeth and at some instants, rotor poles are facing stator slots, so the length between them keeps on changing with respect to the rotor position. Hence, reluctance between them varies according to the rotor position.

The distribution of flux lines for the conventional model and proposed model is shown in Figure 4, which shows the distribution of flux lines at two rotor positions. Figure 4a shows the conventional model rotor position I and Figure 4b shows the proposed model rotor position I. Furthermore, Figure 4c shows the conventional model rotor position II and Figure 4d shows the proposed model rotor position II. Rotor position I in Figure 4a shows the alignment of the rotor core with the upper stator slots and the unalignment with the lower stator slots. Approximately, all the PM flux will flow into the upper air gap due to the maximum reluctance occurring in the lower air gap region. Rotor position I in Figure 4b shows the partial alignment of the rotor core with the upper and lower stator slots. Thus, the PM flux will flow into both the upper and lower air gaps in this case.

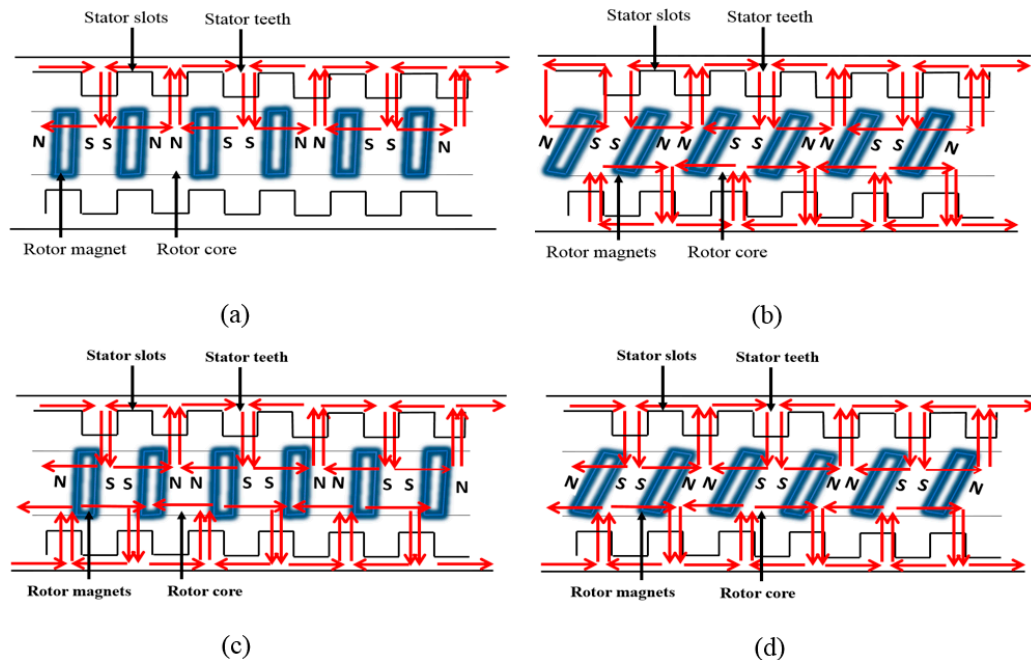


Figure 4. Flux path of the conventional model and proposed model: (a) conventional model position I; (b) proposed model position I; (c) conventional model position II; (d) proposed model position II.

Rotor position II in Figure 4c shows the alignment of the rotor core with the upper and lower stator slots. Approximately, all the PM flux will flow into both of the air gap

regions in this case. Rotor position II in Figure 4d shows the partial alignment of the rotor core with the upper and lower stator slots. Thus, the PM flux will flow into both the upper and lower air gaps in this case. The overall impact of proposed model at both rotor positions I and II has reduced magnetic flux density distribution as well as the gradual change in the reluctance. The reduction in flux density distribution and gradual change in reluctance would result in reduced cogging torque and torque ripple. It is also discussed in the performance analysis Section 3.

2.2. Design of Winding Configuration of DSAFSPMM Machine

The design parameters opted for the conventional DSAFSPMM that is incorporating an unaligned dual stator axial flux spoke-type permanent magnet machine with PGCC winding. For one phase group, the span of the stator teeth and stator slots from the center is the same, i.e., 11.25° mechanical. The span of the slots between the two phases is 15° mechanical. The ratio between the teeth pitch of the same phase and the teeth pitch of the different phases is given by the following equation.

$$\sigma = \frac{\tau_1}{\tau_2} = \frac{\left(\frac{\pi}{2} + \frac{\pi}{2}\right)}{\left(5\frac{\pi}{6} + \frac{\pi}{2}\right)} = \frac{3}{4} \quad (5)$$

where σ represents the ratio between pitches, τ_1 is teeth pitch between two teeth of the same phase, and for the two different phases, teeth pitch between them is τ_2 . For ease of computation, the alternative expression for τ_1 is 3θ and τ_2 is 4θ where θ is expressing the difference between these two pitches as shown in Figure 5.

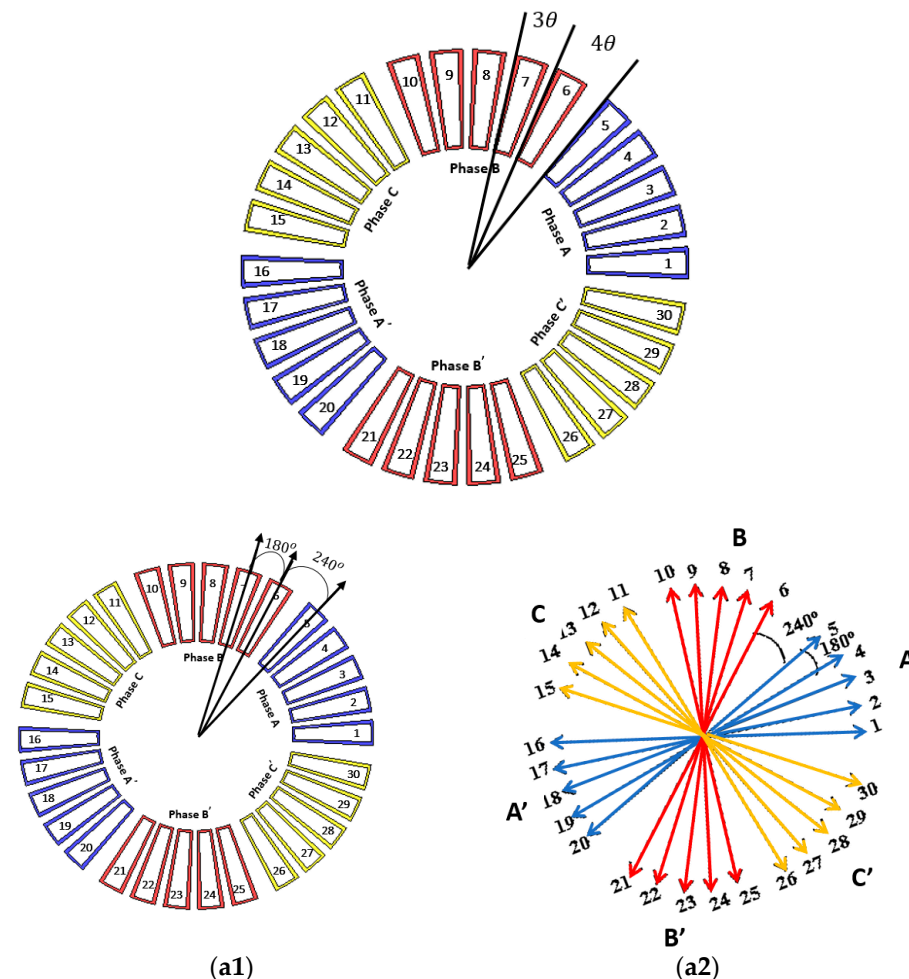


Figure 5. Cont.

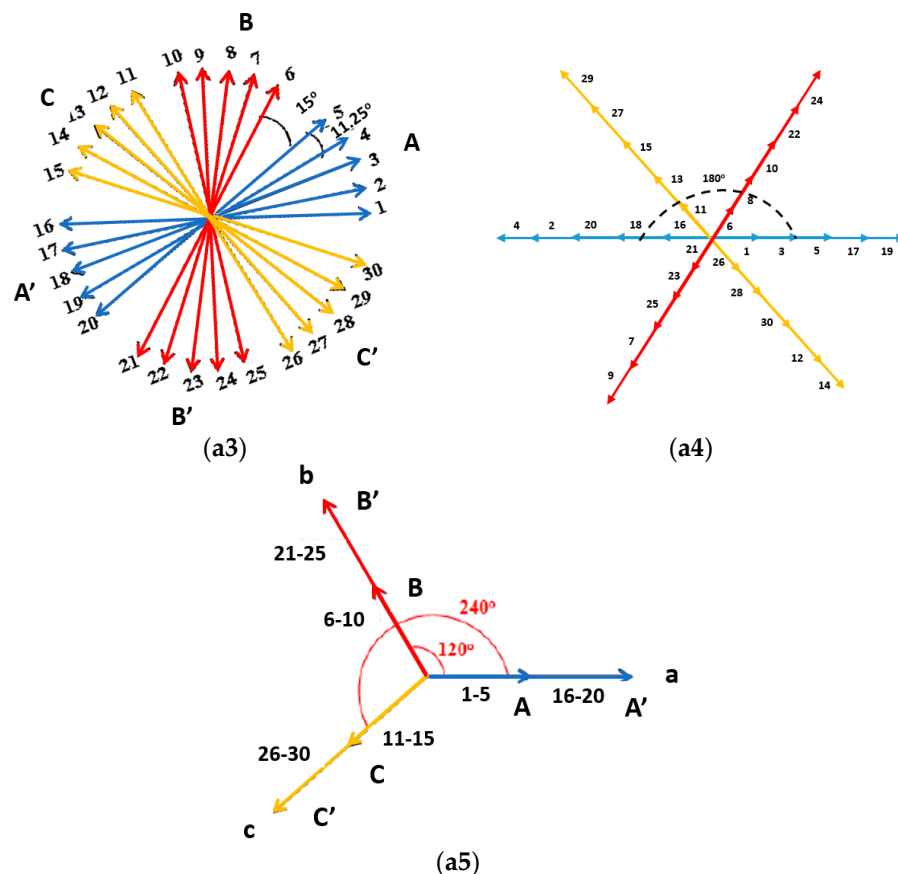


Figure 5. Winding configuration: (a1) 3-phase group winding (elec. deg); (a2) Stator coil (elec. deg); (a3) Stator coils (mech. deg); (a4) EMF vectors; (a5) Resultant EMF vector (elec. deg).

To determine the coil EMF in electrical degrees, the electrical degree (θ_e) can be calculated by the following equation.

$$\theta_e = \frac{P}{2} \theta_m \quad (6)$$

where θ_m is denoting the mechanical degree and P is denoting the number of poles. The conventional winding sequence of stator 1 and stator 2 is shown in Figure 6a. In the conventional coils sequence, stator 1 group of phase A coils (1 to 5) and a group of phase A' coils (16 to 20) are connected in series with stator 2 group of phase A coils (31 to 35) and phase A' coils (46 to 50). Similarly, stator 1 group of phase B coils (6 to 10) and a group of phase B' coils (21 to 25) are connected in series with stator 2 group of phase B coils (36 to 40) and a group of phase B' coils (51 to 55). While stator 1 group of phase C coils (26 to 30) and a group of phase C' coils (11 to 15) are connected in series with stator 2 group of phase C coils (56 to 60) and a group of phase C' coils (41 to 45). Figure 6c shows an equivalent circuit of the conventional winding sequence. The conventional winding sequence is following.

Phase a and Phase a'

Phase b and Phase b'

Phase c and Phase c'

The proposed winding sequence of stator 1 and stator 2 is shown in Figure 6b. In the proposed winding sequence, stator 1 group of phase A coils (1 to 5) and a group of phase A' coils (16 to 20) are connected in series with stator 2 group of phase C coils (55 to 60) and a group of phase C' coils (41 to 45). Similarly, stator 1 group of phase B coils (6 to 10) and a group of phase B' coils (21 to 25) are connected in series with stator 2 group of phase A coils (31 to 35) and a group of phase A' coils (46 to 50). While stator 1 group of phase C coils (26 to 30) and a group of phase C' coils (11 to 15) are connected in series with stator 2 group of phase B coils (36 to 40) and a group of phase B' coils (51 to 55).

coils (26 to 30) and a group of phase C' coils (11 to 15) are connected in series with stator 2 group of phase B coils (36 to 40) and the group of phase B' coils (51 to 55).

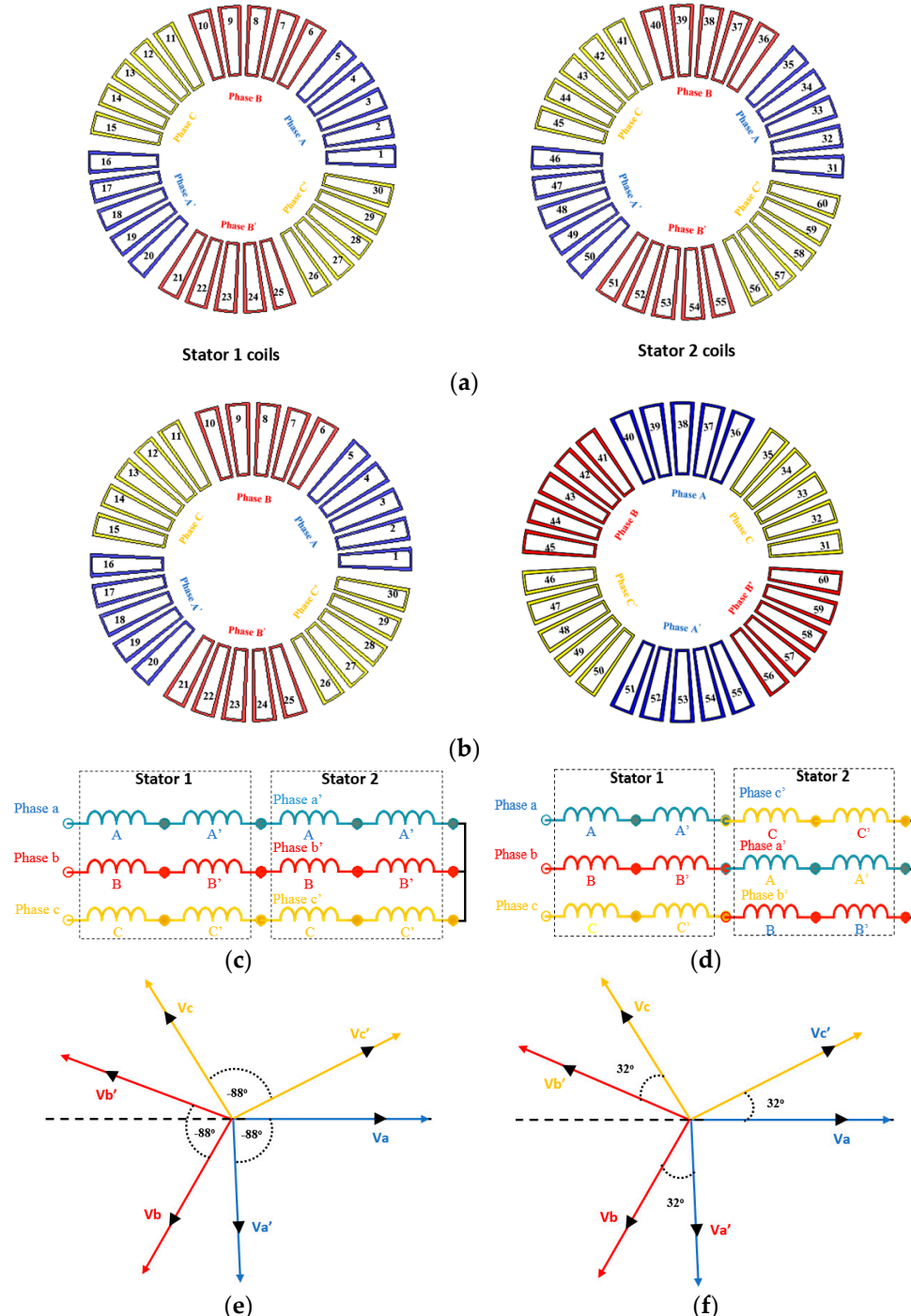


Figure 6. (a) Conventional winding sequence; (b) Proposed winding sequence; (c) Equivalent circuit of conventional winding sequence; (d) Equivalent circuit of proposed winding sequence; (e) Resultant phase difference of conventional winding sequence (elec. deg); (f) Resultant phase difference of proposed winding sequence (elec. deg).

In the proposed winding sequence, stator 1 phases are connected in series with stator 2 phases in such a way that voltage phase shift at positive zero crossing between two phases (stator 1 phase and stator 2 phase) is a minimum of 32° as shown in Figure 6f while phase difference in the conventional winding sequence is 88° as shown in Figure 6e. This reduction in phase difference in the proposed winding sequence improves the distribution factor

which is 0.9613° and ultimately winding factor improves. Whereas the distribution factor in the conventional winding sequence is 0.7192° . The proposed winding sequence ameliorates the voltage magnitude. Hence, the overall average output torque of conventional and proposed models gets better due to the improved distribution factor. This winding sequence also mitigates the voltage total harmonic distortion V_{THD} , significantly. Both proposed models having proposed winding sequence exhibit the least percentage value of V_{THD} due to improved distribution factor that ultimately improves the winding factor. The proposed winding sequence is as follows;

Phase a and Phase c'

Phase b and Phase a'

Phase c and Phase b'

$$K_w = K_p \times K_d \quad (7)$$

$$K_w = K_p \times K_d \quad (8)$$

$$K_w = \cos \frac{\alpha}{2} \times \frac{\sin \frac{m_1 \beta_1}{2}}{m_1 \sin \frac{\beta_1}{2}} \quad (9)$$

$$K_w = \cos \frac{\alpha}{2} \times \frac{\sin \frac{m_2 \beta_2}{2}}{m_2 \sin \frac{\beta_2}{2}} \quad (10)$$

where K_w shows the winding factor, K_p is the pitch factor and K_d is the distribution factor. α is the chording angle in the case of a short pitch coil when the pole pitch is less than or greater than the coil pitch. In the case of full pitch coil $\alpha = 180$ (deg), the pitch factor $\cos \frac{\alpha}{2}$ is equal to 1. While m_1 and m_2 are referring to the no of slots/phase belt as mentioned in Table 1.

The design parameters and materials of the DSAFSPM machine are listed in the form of Table 1, which also describes the materials used for each component in the machine. The rotor and stator part of the machine are made of silicon steel, 50H470 material. The permanent magnets are made of ferrite material, while windings are of copper material. The rotor part is rotating at a constant speed of 480 rpm. The face type mesh element is applied on each part of the machine keeping the constant size element of 2 mm to obtain precise machine 3-D analysis. There are a number of variables that define the machine parameters such as the D_o and D_i denote the outer and inner diameter of the stator and rotor, L_s denotes the total axial length of the machine, h_t and h_y denote the stator tooth and yoke height, respectively, and all the parameters are kept the same for the conventional model, proposed model I and model II. N_c denotes the number of turns per coil, so each coil is utilizing a total number of 36 coils. The air gap for the conventional model, proposed model I and proposed model II is kept the same which is 1 mm, and the total axial length is also the same for all three machines.

The conventional model, proposed model I, and model II machines are sharing same dimensions and incorporate one inner rotor and two outer stators (unaligned) utilizing spoke-type PMs and PGCC winding to enhance the flux-focusing effect on the machine. Exploded views of these machines are shown in Figures 7 and 8, respectively. Adjacent magnets are reversed in polarity by applying outward and inward directions with a circumferentially magnetized pattern. Concentrated coil winding is used in this machine and then the number of groups is made for each phase. Furthermore, neighboring coils within one phase have opposing polarities, which accounts for the alternate magnetization orientations in permanent magnets. Each coil's generated EMF will behave in the same way, following the same direction, resulting in the biggest resultant EMF. The machine topology of the conventional model DSAFSPMM is shown in Figure 7a. The unaligned positioning of both stators is shown in Figure 7b. The machine topology of proposed model I DSAFSPMM and proposed model II DSAFSPMM is shown in Figure 8a,b, respectively.

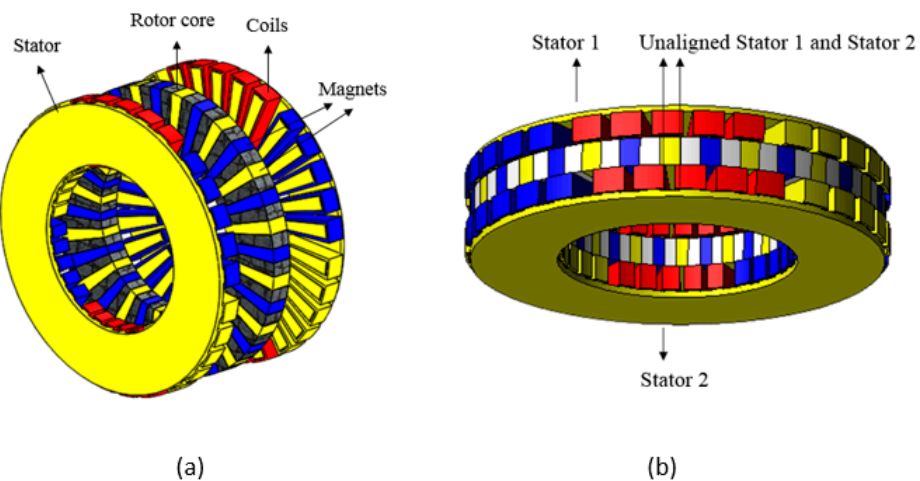


Figure 7. Exploded view of DSAFSPMM with PGCC winding: (a) Conventional model; (b) Unaligned stators in DSAFSPMM.

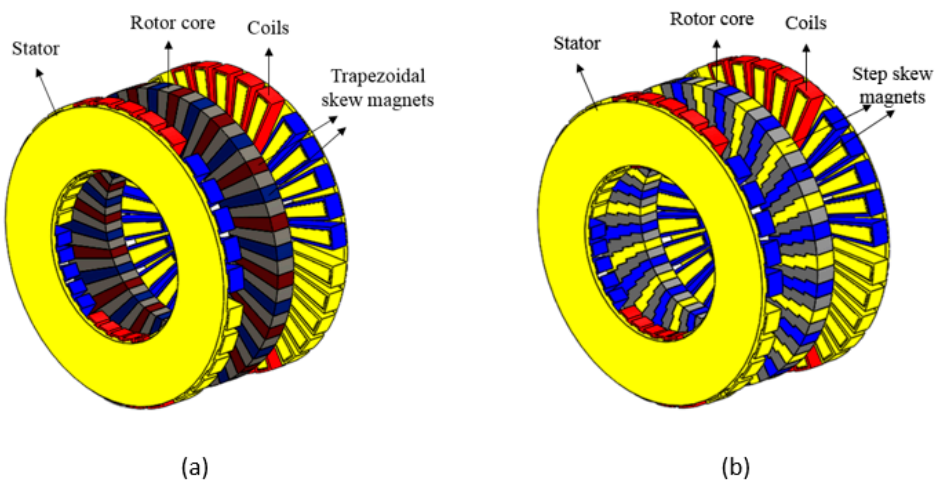


Figure 8. Exploded view of DSAFSPMM with PGCC winding: (a) Proposed model I; (b) Proposed model II.

The summary of the design approach is presented in Figure 9 which describes the machine structure and different techniques that are adopted in the proposed topology to obtain desired results and torque ripple mitigating techniques. Furthermore, the design process is shown in Figure 10 which explains the procedures involved in this research work.

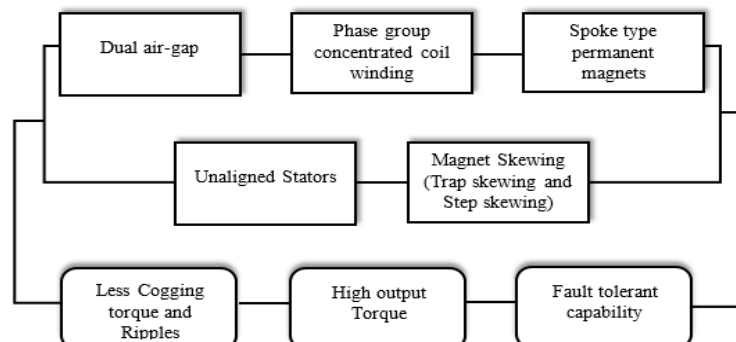


Figure 9. Summary of the design approach to obtain high output torque and reduced torque ripples.

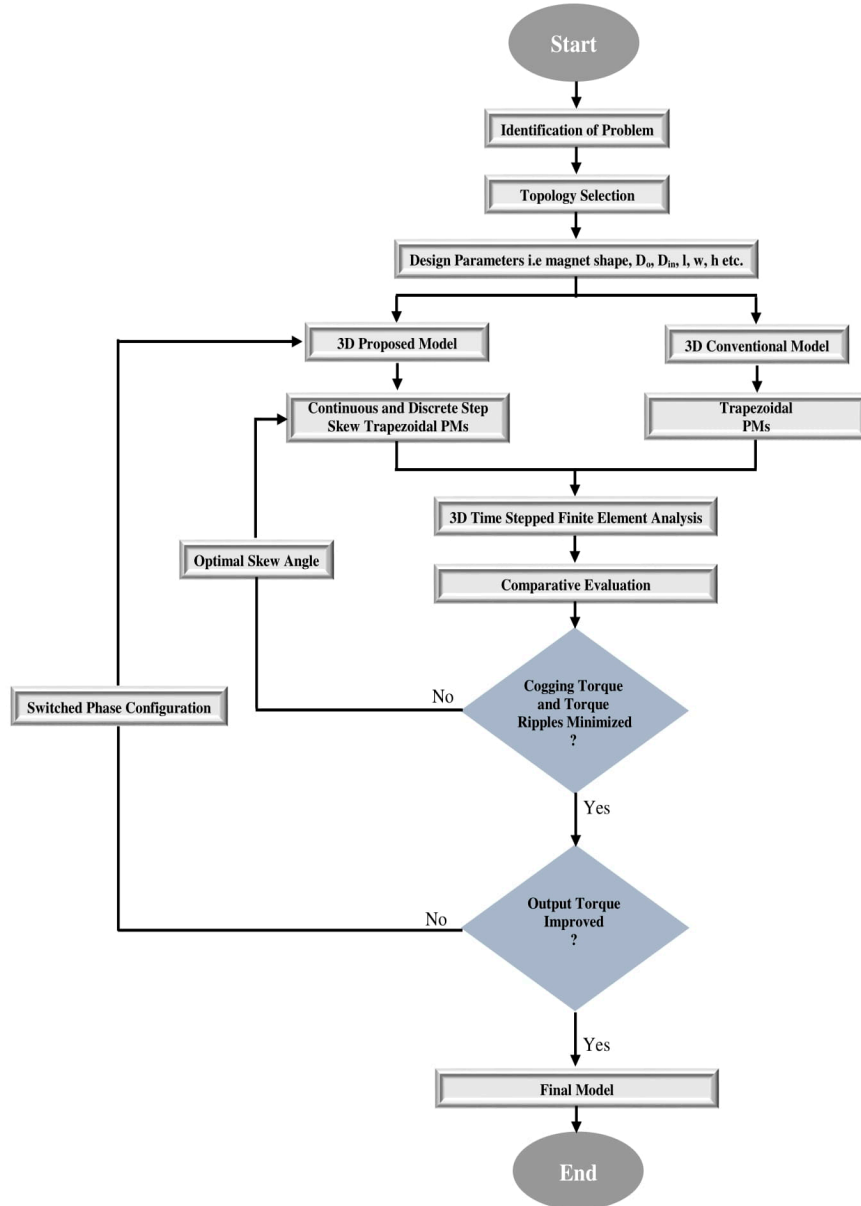


Figure 10. Flow chart of design process.

3. 3-D FEM Analysis

Conventional and proposed model characteristics are analyzed using the 3D time-stepped finite element method to obtain more precise results. This comparative analysis is performed among the conventional model, proposed model I, and proposed model II using the 3D finite element method. This analysis is carried out using the constant volume of the machine as well as the constant volume of conventional and proposed magnets. In this research, time-stepped 3D FEA is used to analyze the cogging torque, output torque, torque ripples, and back EMF of the machines with the conventional and proposed magnets.

Air-Gap Flux Density, PM Flux Linkage, Back EMF, Cogging Torque and Output Torque

A comparative analysis of air gap flux density is shown in Figure 11. The cogging torque is directly proportional to the air gap flux density. The conventional model DSAF-SPM machine has the highest air gap flux density, so cogging torque will be high as compared to proposed model I and proposed model II. There is an inverse relation between air gap flux density and the effective permanence of permanent magnets. The conventional model has lower effective permanence of magnets while proposed model I and proposed

model II have high effective permanence of magnets. As a result, cogging torque will be low in proposed model I and proposed model II. In the conventional model, air-gap flux density (B_g) is 0.8295, while air-gap flux density in proposed model I and proposed model II is 0.7424 and 0.7949, respectively.

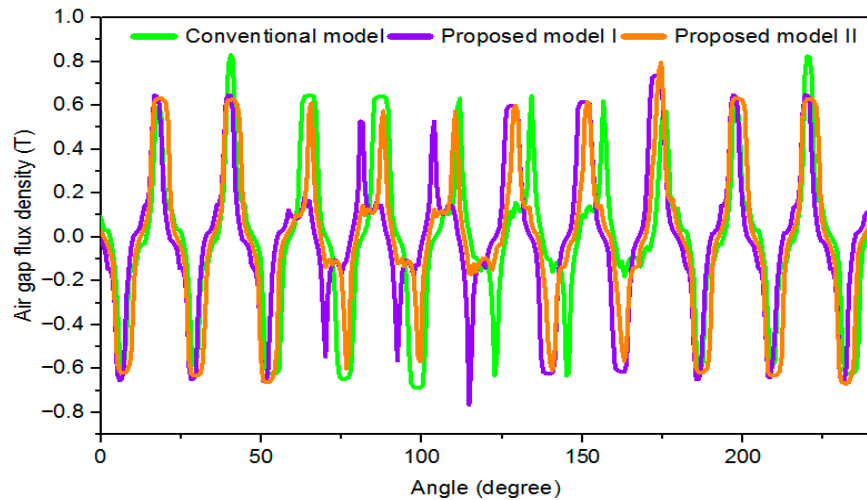


Figure 11. Comparative analysis of air-gap flux density among the conventional model DSAFSPMM, proposed model I DSAFSPMM and proposed model II DSAFSPMM.

The permanent magnet flux linkage of the conventional model, proposed model I, and proposed model II is shown in Figures 12–14, respectively. PM flux linkage is directly related to the output torque of the machine. High flux linkage produces higher output torque. Flux linkage in the conventional model, proposed model I and proposed model II are very close to each other, but the average value of output torque is increased in proposed model I and proposed model II due to fewer ripple factors. This ripple factor is mitigated due to skew techniques in proposed model I and proposed model II because the maximum and minimum value of output torque is reduced so less ripple factor will involve. Torque ripple is a periodic increase or decrease in output torque as the motor shaft rotates. It is measured as the ratio of the difference in the maximum and minimum torque to the average torque and is generally expressed as a percentage. The flux linkage of the conventional model is 0.05856, while the flux linkage of proposed model I and proposed model II is 0.05885 and 0.05965.

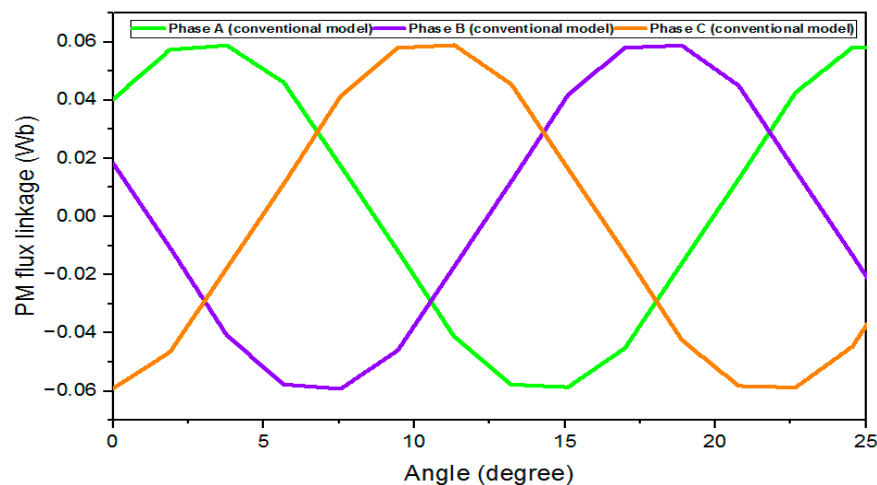


Figure 12. PM flux linkage of the conventional model DSAFSPMM.

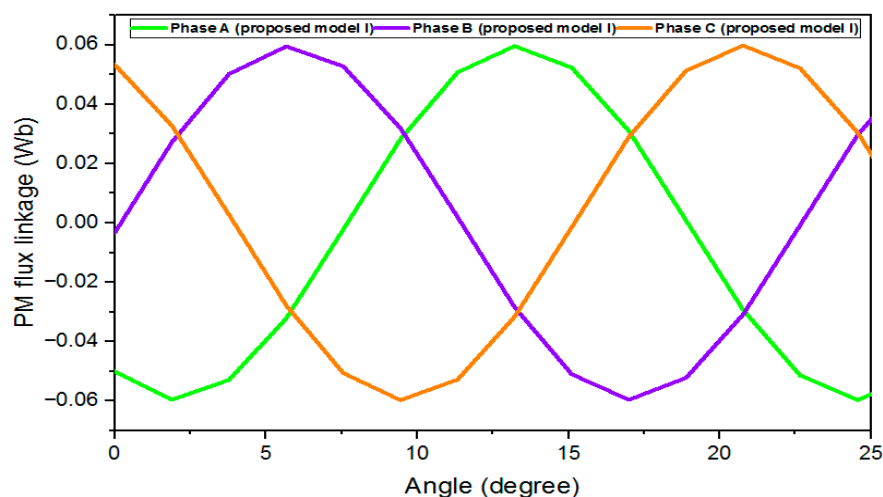


Figure 13. PM flux linkage of proposed model I DSAFSPMM.

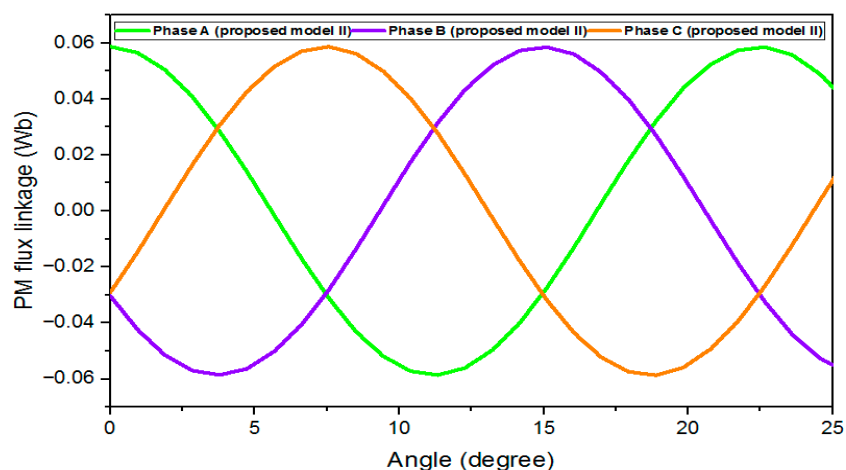


Figure 14. PM flux linkage of proposed model II DSAFSPMM.

Phase back EMF of the conventional model and proposed model I is shown in Figure 15. It can be noticed in Figure 15 that the back EMF of proposed model I is more sinusoidal as compared to the conventional model due to the continuous skew in magnet shape. The back EMF of the conventional model is $138.5 \text{ V}_{\text{rms}}$, which is slightly greater than that of proposed model I which is $132.4 \text{ V}_{\text{rms}}$. Phase back EMF of the conventional model and proposed model II is shown in Figure 16. It shows that the back EMF of proposed model II is more sinusoidal as compared to the conventional model due to the discrete step-skew magnets which mitigates the harmonic components significantly. The back EMF of the conventional model is $138.5 \text{ V}_{\text{rms}}$, while that of proposed model II is $124.09 \text{ V}_{\text{rms}}$. Proposed model I and proposed model II have more sinusoidal back EMF as compared to the conventional model due to the lower V_{THD} percentage.

A comparative analysis of cogging torque among the three DSAFSPMM models, conventional model, proposed model I, and proposed model II is shown in Figure 17. In this analysis, it is noticed that there is a significant difference in cogging torque with and without the skew shape of the magnet. The conventional model has 20 Nm peak-to-peak cogging torque, while proposed model I has 3.7 Nm peak-to-peak cogging torque and proposed model II has 5 Nm peak-to-peak cogging torque. The machine that is utilizing the continuous skew magnet technique mitigates the overall cogging torque up to 81.5% while the machine that is utilizing the discrete step-skew magnet technique mitigates the cogging torque up to 75% . This reduction in cogging torque reduces the noise and vibration in machines which assists the machines to perform smooth operations.

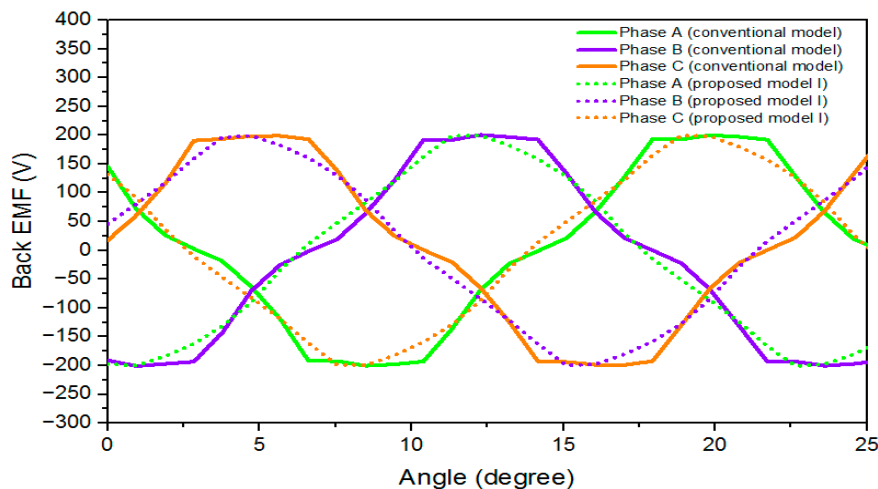


Figure 15. Phase back EMF of conventional model DSAFSPMM and proposed model I DSAFSPMM.

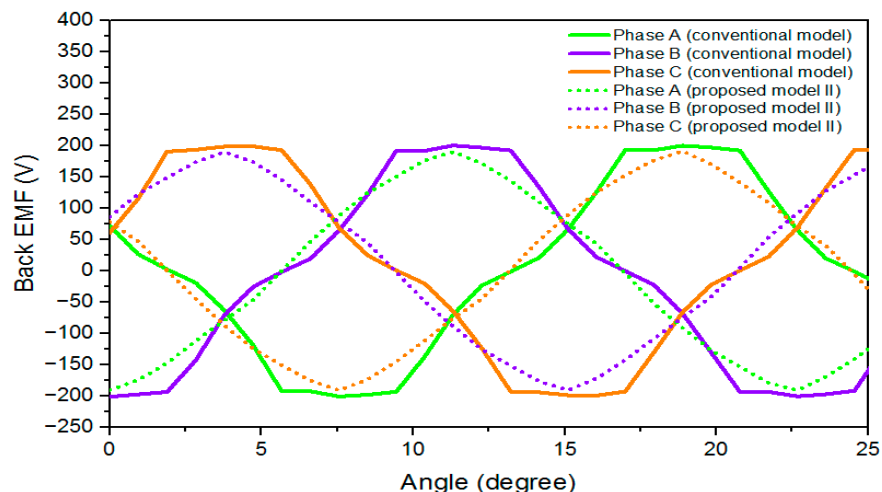


Figure 16. Phase back EMF of conventional model DSAFSPMM and proposed model II DSAFSPMM.

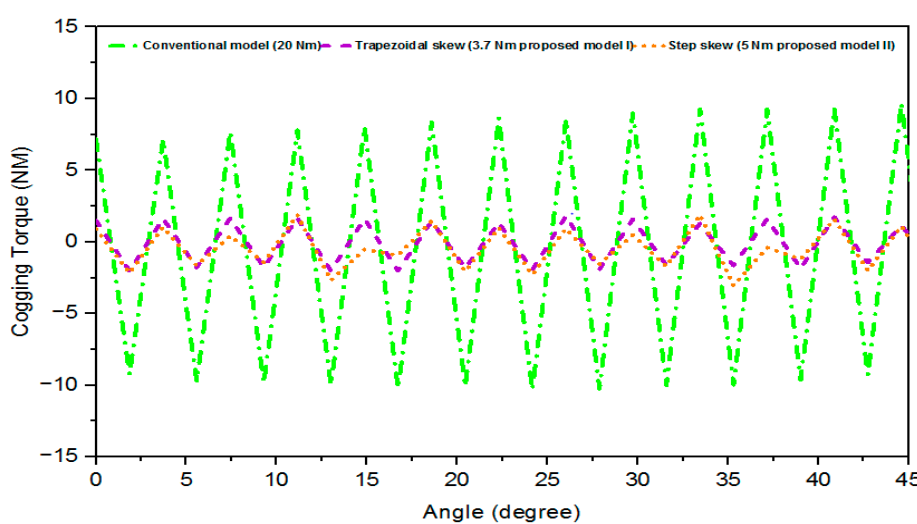


Figure 17. Comparative analysis of cogging torque among conventional model DSAFSPMM, proposed model I DSAFSPMM and proposed model II DSAFSPMM.

A comparative analysis of average output torque for the conventional winding sequence among the three DSAFSPMM models, conventional model, proposed model I, and

proposed model II is shown in Figure 18. Analysis shows that there is a considerable difference between average output torque and the output torque ripples with and without the skew shape of magnets. Output torque ripples are reduced in proposed model I and proposed model II due to the decrease in cogging torque and improved sinusoidal back EMF of the machines. Harmonic components are also reduced significantly. The conventional model has 53 Nm average output torque, while proposed model I has 61 Nm average output torque and proposed model II has 65 Nm average output torque.

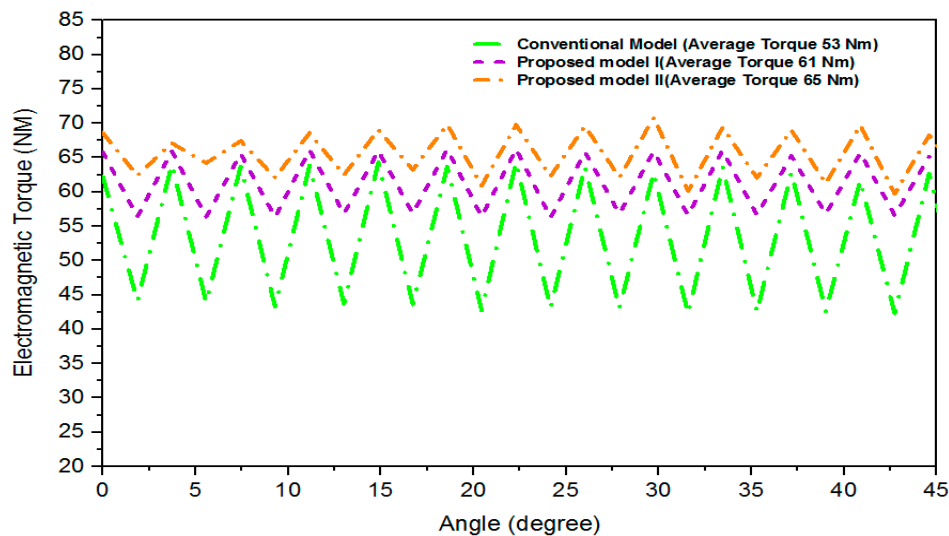


Figure 18. Comparative analysis of average output torque and torque ripples among conventional model DSAFSPMM, proposed model I DSAFSPMM and proposed model II DSAFSPMM.

Torque ripple is a periodic increase or decrease in output torque as the motor shaft rotates. It is measured as the ratio of the difference in maximum and minimum torque to the average torque and is generally expressed as a percentage.

$$\tau_{ripples} = \frac{\tau_{max} - \tau_{min}}{\tau_{avg}} \times 100 \quad (11)$$

The conventional model has 41.6% output torque ripples. Whereas proposed model I has 16.3% torque ripples and proposed model II has 16.9% torque ripples. Reduction in output torque ripples in proposed model I is 60.8% as compared to the conventional model, while that of proposed model II is 59.3%. Further improvement in output torque is made by switching winding sequences of both stator coils.

Core losses are a combination of stator loss and rotor loss while copper loss includes winding loss. Copper loss for the conventional model, proposed model I and proposed model II is 125 W while iron losses for the conventional model, proposed model I and proposed model II are 58 W, 41 W and 41 W, respectively. The conventional model efficiency is 93.6% while proposed model I, and proposed model II efficiency is 94.8% and 95.1%, respectively, as shown in Table 2. Efficiency is calculated by the following equation.

$$\text{Efficiency} = \frac{\tau \times \omega}{(\tau \times \omega) + \text{copper loss} + \text{iron loss}} \times 100$$

where τ is the average torque of the machine and ω is the rotational speed of the machine. While copper loss and iron loss are given in Table 2.

Table 2. Performance comparison of conventional model DSAFSPMM, proposed model I DSAFSPMM and proposed model II DSAFSPMM with conventional winding sequence.

Item	Units	Conventional Model (DSAFTSPM) Machine	Proposed Model I (DSAFTSPM) Machine	Proposed Model II (DSAFTSPM) Machine
Cogging torque (peak to peak)	Nm	20	3.7	5
Output torque (AVG)	Nm	53.3	61.3	65
Torque ripple factor	%	41.6	16.3	16.9
Phase back EMF (RMS)	V	138.50	132.46	124.09
V_{THD}	%	11.2514	6.7869	4.6050
B_g	T	0.8295	0.7424	0.7849
Copper loss	W	125.5	125.5	125.5
Iron loss	W	58	41	41
Efficiency	%	93.6	94.8	95.1

Phase back EMF of conventional model DSAFSPMM with the proposed winding sequence is shown in Figure 19. It can be noticed in Figure 19 that back EMF is significantly increased from $138.5 \text{ V}_{\text{rms}}$ to $182.6 \text{ V}_{\text{rms}}$ and is relatively more sinusoidal as compared to the conventional winding sequence. This phase back EMF is improved by 24.1% as compared to the conventional winding sequence.

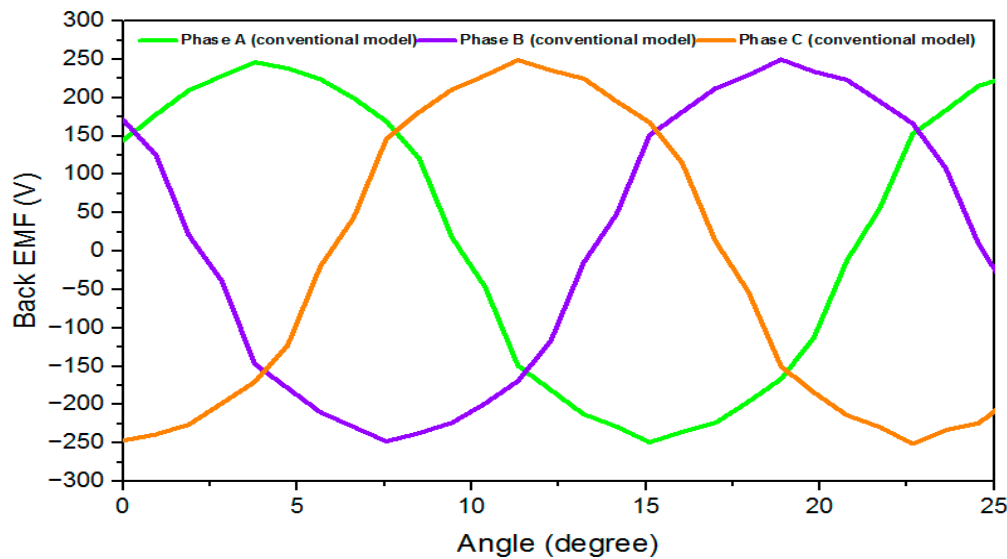


Figure 19. Phase back EMF of conventional model DSAFSPMM with proposed winding sequence.

Phase back EMF of proposed model I DSAFSPMM with the proposed winding sequence is shown in Figure 20. It shows that the back EMF is significantly improved from $132.4 \text{ V}_{\text{rms}}$ to $162.02 \text{ V}_{\text{rms}}$ and is relatively more sinusoidal as compared to the conventional winding sequence. This phase back EMF is ameliorated by 18.2%. Furthermore, phase back EMF of proposed model II DSAFSPMM with the proposed winding sequence is shown in Figure 21. It can be noticed in Figure 21 that back EMF is significantly increased from $124.09 \text{ V}_{\text{rms}}$ to $162.86 \text{ V}_{\text{rms}}$ and is relatively more sinusoidal as compared to the conventional winding sequence. This phase back EMF is ameliorated by 23.8%.

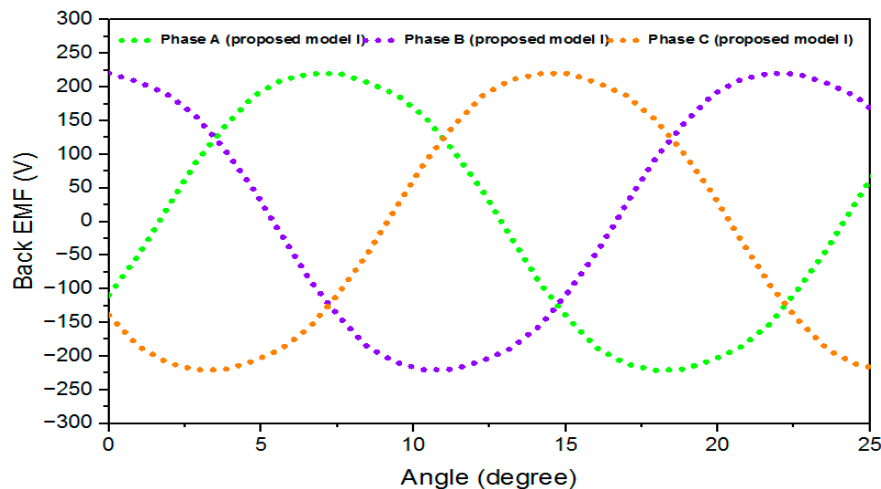


Figure 20. Phase back EMF of proposed model I DSAFSPMM with proposed winding sequence.

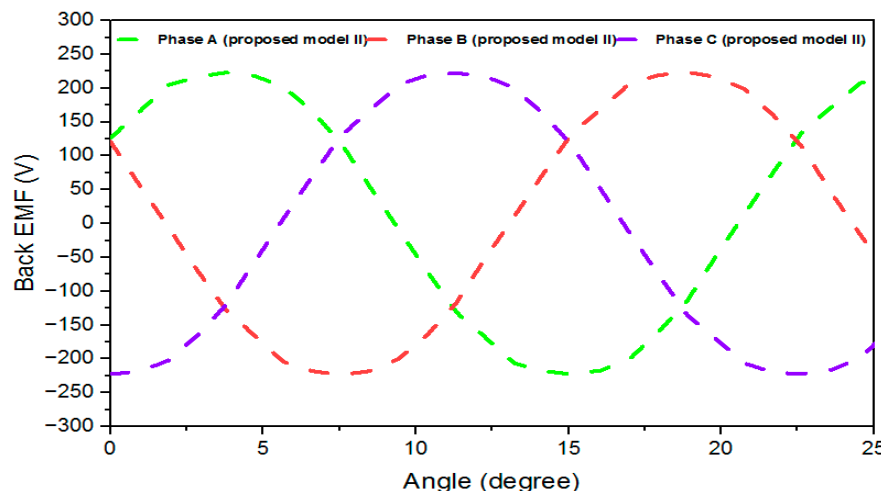


Figure 21. Phase back EMF of proposed model II DSAFSPMM with proposed winding sequence.

By using the proposed winding sequence, V_{THD} is decreased from 11.25% to 8.42% which is an improvement of 25.2%. While proposed model I and proposed model II with the proposed winding sequence, mitigate V_{THD} from 6.78% to 3.93% and from 4.76% to 3.66% respectively, which improves V_{THD} by 42% and 23 % in proposed model I and proposed model II, respectively. Figure 22 presents the voltage total harmonic distortion in the form of percentage for the conventional and proposed models, where A', B', and C' denote the conventional model, proposed model I, and proposed model II, respectively.

A comparative analysis of average output torque for conventional model DSAFSPMM with proposed winding sequence and conventional winding sequence is shown in Figure 23. In this analysis, it is noticed that there is a significant difference in average output torque using the proposed winding sequence. The average output torque for the conventional DSAFSPMM with the conventional winding sequence is 53 NM while the average output torque by using the proposed winding sequence for the conventional DSAFSPMM is 94 NM. This average output torque is improved by 43.6% as compared to the conventional winding sequence due to the improved distribution factor K_d . Output torque ripples of the conventional model with a conventional winding sequence are 41.6% while output torque ripples using the proposed winding sequence are 16.5%.

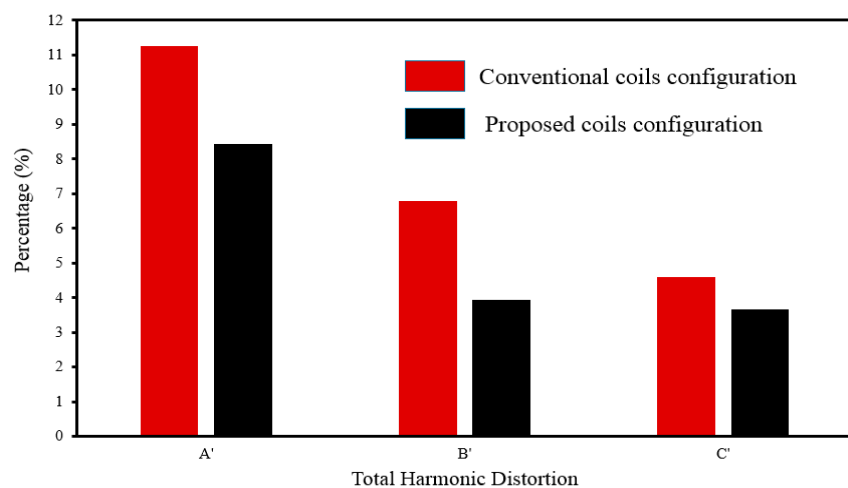


Figure 22. Total harmonic distortion percentage with conventional and proposed winding sequence.

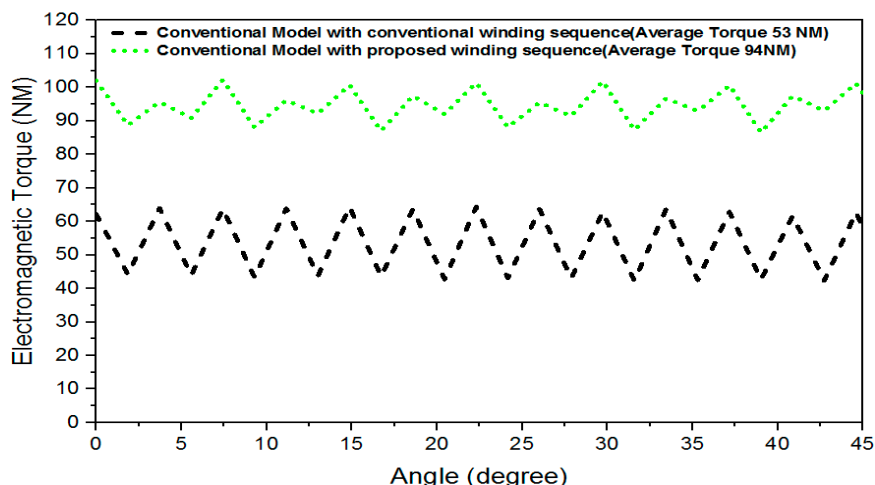


Figure 23. Comparative analysis of average output torque for conventional model DSAFSPMM using conventional and proposed winding sequence.

A comparative analysis of average output torque for proposed model I DSAFSPMM with the proposed winding sequence and the conventional winding sequence is shown in Figure 24. The average output torque for proposed model I DSAFSPMM with a conventional winding sequence is 61 NM while the average output torque for proposed model I DSAFSPMM with the proposed winding sequence is 82 NM. This average output torque is improved by 25.6%. Output torque ripples value using conventional winding sequence is 16.3% while output torque ripples value using proposed winding sequence is only 6%. The reduction in torque ripple using the proposed winding sequence is 63.1%.

For proposed model II DSAFSPMM, a comparative analysis of average output torque with the proposed winding sequence and conventional winding sequence is shown in Figure 25. The average output torque of proposed model II DSAFSPMM with the conventional winding sequence is 65 NM while the average output torque of proposed model II DSAFSPMM with the proposed winding sequence is 84 NM. This average output torque is improved by 22.6%. The output torque ripples value using a conventional winding sequence is 16.9% while the output torque ripples value using the proposed winding sequence is only 16.5%.

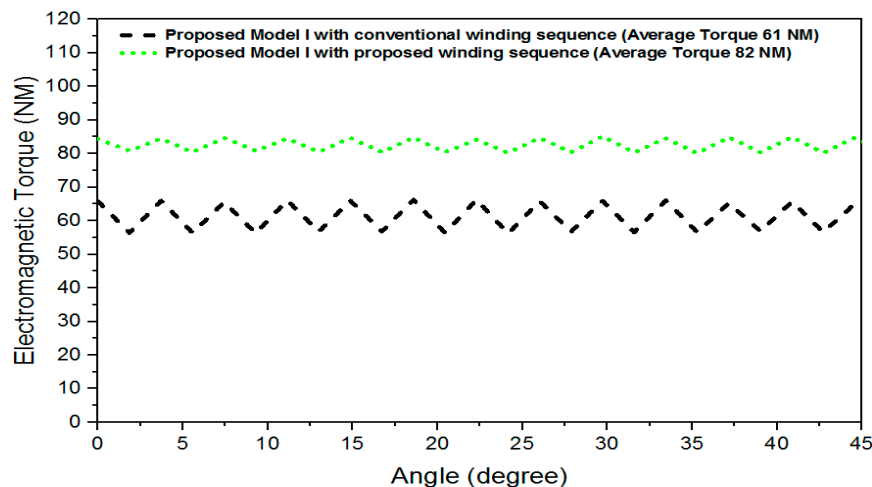


Figure 24. Comparative analysis of average output torque for proposed model I DSAFSPMM with conventional and proposed winding sequence.

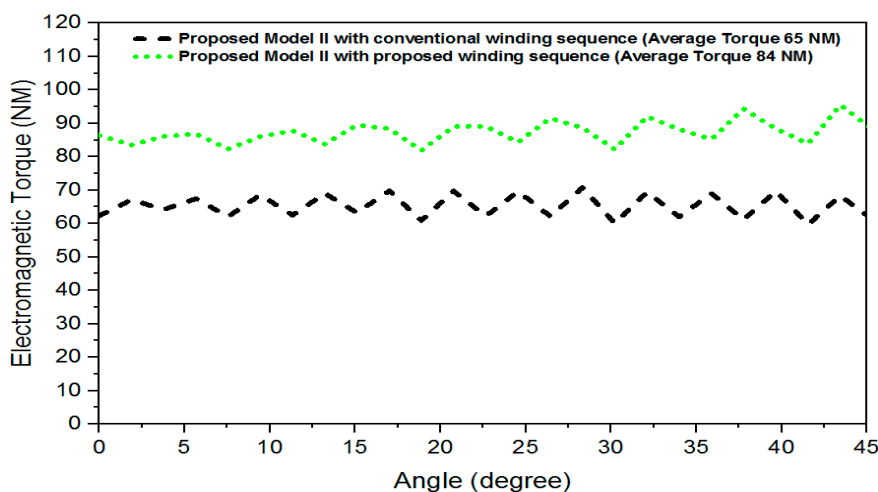


Figure 25. Comparative analysis of average output torque for proposed model II DSAFSPMM with conventional and proposed winding sequence.

4. Conclusions

In this paper, two dual stator axial flux spoke-type permanent magnet machines are proposed, one of them uses continuously skewed and the other one uses discrete step-skewed rotor magnets. These machines utilize PGCC windings and cost-effective ferrite PMs are inserted into the rotor in the form of spoke-type array to increase the flux-focusing effect. Based on the 3D time-stepped finite element analysis, the comparative analysis shows that continuous skew trapezoidal magnets and discrete step-skew trapezoidal magnets have a significantly lower value of cogging torque and torque ripples as compared to no skew trapezoidal magnets. The reason behind the reduction in cogging torque is that the cogging effects from the magnets are out of phase with each other.

The cogging torque and torque ripples using continuous skew magnets are mitigated by 85% and 60.8%, respectively, while cogging torque and torque ripples using discrete step-skew magnets, are mitigated by 75% and 59.3%, respectively as compared to the conventional model which uses no skew PMs. The back EMF of proposed models is more sinusoidal as compared to the conventional model. Further improvement in back EMF and output torque is achieved by switching the winding sequence. By the proposed winding sequence, the output torque of the conventional model is improved by 43% as compared to the conventional coils winding sequence while output torque with the continuous trapezoidal skew magnet and discrete step-skew trapezoidal magnet is improved by 25.6%.

and 22.6%, respectively. The performance comparison of conventional model DSAFSPMM, proposed model I DSAFSPMM and the proposed model II DSAFSPMM with proposed winding sequence is shown in Table 3. Therefore, three-phase axial flux spoke-type PM machines having continuous skewing and discrete step-skewing magnets with the proposed winding sequence are proposed to ameliorate the machine performance.

Table 3. Performance comparison of conventional model DSAFSPMM, proposed model I DSAFSPMM and proposed model II DSAFSPMM with proposed winding sequence.

Item	Units	Conventional Model (DSAFTSPM) Machine	Proposed Model I (DSAFTSPM) Machine	Proposed Model II (DSAFTSPM) Machine
Cogging torque (peak to peak)	Nm	20	3.7	5
Output torque (AVG)	Nm	94	82	84
Torque ripple factor	%	16.5	6	16.5
Phase back EMF (RMS)	V	182.60	162.02	162.86
V_{THD}	%	8.4260	3.9371	3.6695
Copper loss	W	125.5	125.5	125.5
Iron loss	W	58	41	41
Efficiency	%	96.2	96.1	96.2

Author Contributions: Conceptualization, M.R.Z., J.I. and F.M.; methodology, S.S.H.B., J.I. and S.A.; software, M.R.Z., S.I.S. and S.A.; validation, M.R.Z., S.A., and J.I.; formal analysis, F.M.; investigation, J.I. and S.S.H.B.; resources, F.M.; writing—original draft preparation, M.R.Z., S.I.S.; writing—review and editing, F.M. and S.A.; visualization, M.R.Z. and S.S.H.B.; supervision, F.M.; project administration, F.M.; funding acquisition, F.M. All authors have read and agreed to the published version of the manuscript.

Funding: The authors recognize the financial support of Regione Lazio through LazioInnova’s “Progetti di Gruppi di Ricerca, Conoscenza e Cooperazione per un Nuovo Modello di Sviluppo finanziati ai sensi della L.R. Lazio 13/08”. The Project of excellence of the department of Electrical and Information Engineering, University of Cassino and Southern Lazio on “Intelligent distributed systems”.

Data Availability Statement: Not applicable.

Acknowledgments: The authors acknowledge the support of the Italian Ministry of Education (MUR) through the Project of Excellence of the Department of Electrical and Information Engineering of the University of Cassino and Southern Lazio on “Intelligent distributed systems” and the financial support of Regione Lazio through LazioInnova’s “Progetti di Gruppi di Ricerca, Conoscenza e Cooperazione per un Nuovo Modello di Sviluppo finanziati ai sensi della L.R. Lazio 13/08”.

Conflicts of Interest: The authors declare no conflict of interest.

References

1. Kimiaiegi, M.; Widmer, J.D.; Long, R.; Gao, Y.; Goss, J.; Martin, R.; Lisle, T.; Vizan, J.M.S.; Michaelides, A.; Mecrow, B. High-Performance Low-Cost Electric Motor for Electric Vehicles Using Ferrite Magnets. *IEEE Trans. Ind. Electron.* **2015**, *63*, 113–122. [[CrossRef](#)]
2. Chen, Y.; Pillay, P.; Khan, A. PM wind generator topologies. *IEEE Trans. Ind. Appl.* **2005**, *41*, 1619–1626. [[CrossRef](#)]
3. Li, Y.; Yang, H.; Lin, H.; Fang, S.; Wang, W. A Novel Magnet-Axis-Shifted Hybrid Permanent Magnet Machine for Electric Vehicle Applications. *Energies* **2019**, *12*, 641. [[CrossRef](#)]
4. Ismagilov, F.R.; Papini, L.; Vavilov, V.E.; Gusakov, D.V. Design and Performance of a High-Speed Permanent Magnet Generator with Amorphous Alloy Magnetic Core for Aerospace Applications. *IEEE Trans. Ind. Electron.* **2020**, *67*, 1750–1758. [[CrossRef](#)]
5. Kim, S.; Cho, J.; Park, S.; Park, T. Characteristics comparison of a conventional and modified spoke-type ferrite magnet motor for traction drives of low-speed. *IEEE Trans. Ind. Appl.* **2013**, *49*, 2516–2523. [[CrossRef](#)]
6. Du, Z.S.; Lipo, T.A. Design of an Improved Dual-Stator Ferrite Magnet Vernier Machine to Replace an Industrial Rare-Earth IPM Machine. *IEEE Trans. Energy Convers.* **2019**, *34*, 2062–2069. [[CrossRef](#)]

7. Amin, S.; Khan, S.; Bukhari, S.S.H. A Comprehensive Review on Axial Flux Machines and Its Applications. In Proceedings of the 2nd International Conference on Computing, Mathematics & Engineering Technologies (iCoMET 2019), Sukkur, Pakistan, 30–31 January 2019; pp. 1–7. [[CrossRef](#)]
8. Kwon, J.-W.; Lee, J.-H.; Zhao, W.; Kwon, B.-I. Flux-Switching Permanent Magnet Machine with Phase-Group Concentrated-Coil Windings and Cogging Torque Reduction Technique. *Energies* **2018**, *11*, 2758. [[CrossRef](#)]
9. Baig, M.A.; Ikram, J.; Iftikhar, A.; Bukhari, S.S.H.; Khan, N.; Ro, J.-S. Minimization of Cogging Torque in Axial Field Flux Switching Machine Using Arc Shaped Triangular Magnets. *IEEE Access* **2020**, *8*, 227193–227201. [[CrossRef](#)]
10. Di Gerlando, A.; Foglia, G.; Iacchetti, M.F.; Perini, R. Axial flux PM machines with concentrated armature windings: Design analysis and test validation of wind energy generators. *IEEE Trans. Ind. Electron.* **2010**, *58*, 3795–3805. [[CrossRef](#)]
11. Ali, R.; Amjadullah; Ali, S.; Ullah, H. Cogging-Torque Reduction Techniques in Axial Flux Permanent Magnet Machine. *Int. J. Eng. Work.* **2021**, *8*, 262–266. [[CrossRef](#)]
12. Wang, X.; Sun, X.; Gao, P. Study on the effects of rotor-step skewing on the vibration and noise of a PMSM for electric vehicles. *IET Electr. Power Appl.* **2020**, *14*, 131–138. [[CrossRef](#)]
13. Zhao, W.; Lipo, T.A.; Kwon, B.-I. Dual-stator Two-phase Permanent Magnet Machines with Phase-group Concentrated-coil Windings for Torque Enhancement. *IEEE Trans. Magn.* **2015**, *51*, 8112404. [[CrossRef](#)]
14. Zhao, W.; Chen, D.; Lipo, T.A.; Kwon, B.-I. Dual Airgap Stator- and Rotor-Permanent Magnet Machines With Spoke-Type Configurations Using Phase-Group Concentrated Coil Windings. *IEEE Trans. Ind. Appl.* **2017**, *53*, 3327–3335. [[CrossRef](#)]
15. Ying, H.; Zhang, Z.; Gong, J.; Huang, S.; Ding, X. Application for Step-skewing of Rotor of IPM Motors Used in EV. *World Electr. Veh. J.* **2011**, *4*, 532–536. [[CrossRef](#)]
16. Zhao, W.; Lipo, T.A.; Kwon, B.-I. Design and analysis of a novel dual stator axial flux spoke-type ferrite permanent magnet machine. In Proceedings of the IECON 2013—39th Annual Conference of the IEEE Industrial Electronics Society, Vienna, Austria, 10–13 November 2013; pp. 2714–2719. [[CrossRef](#)]
17. Zhao, W.; Lipo, T.A.; Kwon, B.-I. Torque Pulsation Minimization in Spoke-type Interior Permanent Magnet Motors With Skewing and Sinusoidal Permanent Magnet Configurations. *IEEE Trans. Magn.* **2015**, *51*, 8110804. [[CrossRef](#)]
18. Li, Y.; Yang, H.; Lin, H.; Lyu, S.; Pan, Z. Comparative Study of Stator-Consequent-Pole Permanent Magnet Machines With Different Stator-Slot Configurations. *IEEE Trans. Magn.* **2019**, *55*, 8106308. [[CrossRef](#)]
19. Aydin, M.; Gulec, M. Reduction of Cogging Torque in Double-Rotor Axial-Flux Permanent-Magnet Disk Motors: A Review of Cost-Effective Magnet-Skewing Techniques With Experimental Verification. *IEEE Trans. Ind. Electron.* **2014**, *61*, 5025–5034. [[CrossRef](#)]
20. Gundogdu, T.; Komurgoz, G. Design of Permanent Magnet Machines with Different Rotor Type. In Internation General of Electrical and Computer Engineering World Academy of Science, Engineering and Technology. *Int. J. Electr. Comput. Eng.* **2010**, *4*, 10.
21. Ge, X.; Zhu, Z. Optimal Step-Skew Methods for Cogging Torque Reduction Accounting for Three-Dimensional Effect of Interior Permanent Magnet Machines. *IEEE Trans. Energy Convers.* **2017**, *32*, 222–232. [[CrossRef](#)]
22. Sikder, C.; Husain, I.; Ouyang, W. Cogging Torque Reduction in Flux-Switching Permanent-Magnet Machines by Rotor Pole Shaping. *IEEE Trans. Ind. Appl.* **2015**, *51*, 3609–3619. [[CrossRef](#)]
23. Kim, S.-A.; Choi, G.-D.; Lee, J.; Cho, Y.-H. Optimal rotor shape design of 3-step skew spoke type BLAC motor to reducing cogging torque. *Int. J. Appl. Electromagn. Mech.* **2016**, *51*, S135–S145. [[CrossRef](#)]
24. Blum, J.; Merwerth, J.; Herzog, H.-G. Investigation of the segment order in step-skewed synchronous machines on noise and vibration. In Proceedings of the 2014 4th International Electric Drives Production Conference (EDPC), Nuremberg, Germany, 30 September–1 October 2014. [[CrossRef](#)]